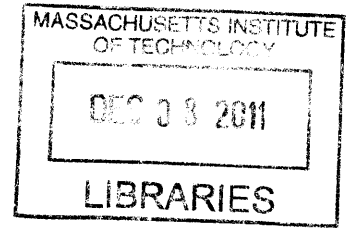


RattleSnake: Stochastic Folding for Chain Programmable Matter

by

Maxim B. Lobovsky

B.S. Applied and Engineering Physics
Cornell University, 2009



ARCHIVES

Submitted to the Program in Media Arts and Sciences,
School of Architecture and Planning,
in partial fulfillment of the requirements for the degree of
Master of Science in Media Arts and Sciences
at the
MASSACHUSETTS INSTITUTE OF TECHNOLOGY
September 2011

© Massachusetts Institute of Technology 2011. All rights reserved.

Author

Maxim Lobovsky
Program in Media Arts and Sciences
August 19, 2011

Certified by

Neil Gershenfeld
Professor of Media Arts and Sciences
MIT Center for Bits and Atoms
Thesis Supervisor

Accepted by

Mitchel Resnick
LEGO Papert Professor of Learning Research
Academic Head
Program in Media Arts and Sciences

RattleSnake: Stochastic Folding for Chain Programmable Matter

by

Maxim B. Lobovsky

Submitted to the Program in Media Arts and Sciences,
School of Architecture and Planning,
on August 19, 2011, in partial fulfillment of the
requirements for the degree of
Master of Science in Media Arts and Sciences

ABSTRACT

The vision of programmable matter is to create a blob of material that can transform itself into an arbitrary form. One promising approach for achieving programmable matter is to construct a chain of identical nodes that can fold into arbitrary three-dimensional shapes. Previous active electromechanical systems have demonstrated this concept but are currently costly, complex, and not robust enough to scale to smaller sizes or larger numbers of nodes.

The goal of this thesis is to explore methods of simplifying chain programmable matter by removing the actuator from each node and, instead, putting energy into the system externally through stochastic vibrations. Each node takes this random energy input and rectifies it to produce motion towards the target position. We propose two variants of this system: 1) smart clutches that can be reprogrammed in situ and fold through arbitrary paths in configuration space and 2) ratchets that are programmed ahead of time and are entirely passive. We developed a chain using the ratchet concept and also constructed a new active, electromechanical chain with reduced cost and improved speed and torque compared to previous electromechanical systems. Through experimental and computer simulated studies, we determined that stochastic actuation can simplify and reduce the cost of these systems. We have also identified how the size of the increments of the ratchet, length of the chain, and the amplitude and frequency of agitation affect the folding time and success rate. In addition, we show that passive folding systems should improve in performance as the hardware scales down.

Thesis Supervisor:
Neil Gershenfeld
Professor of Media Arts and Sciences

The material in this thesis was also based upon work supported by, or in part by, the U. S. Army Research Laboratory and the U. S. Army Research Office under contract/grant number W911NF-08-1-0254.

RattleSnake: Stochastic Folding for Chain Programmable Matter

by

Maxim B. Lobovsky

The following person served as a reader for this thesis:

Thesis reader _____

Joseph Jacobson

Associate Professor of Media Arts and Sciences
MIT Media Laboratory and Center for Bits and Atoms

RattleSnake: Stochastic Folding for Chain Programmable Matter

by

Maxim B. Lobovsky

The following person served as a reader for this thesis:

Thesis reader

Jonathan Bachrach
Research Scientist
Other Lab

ACKNOWLEDGMENTS

To Professor Neil Gershenfeld thanks for accepting me into your incredible group of computer scientists, physicists, engineers, architects and artists. I do not believe there is any other place in the world where I could get access to such an amazing mix of people, tools, resources, and interesting projects. Though at times I struggled against it, your instinct about when to throw out conventional wisdom has helped me become more creative and adventurous in my work.

To Professor Joe Jacobson, every conversation I have had with you has been enlightening. I would have greatly enjoyed the chance to spend more time with you.

To Jonathan Bachrach, thank you for all the great brainstorming sessions, and your help on all of my work, especially with the simulation aspect of this thesis. Also, thanks for lending a bit of California sun and relaxation to me here in Boston even remotely over video conferences.

To the undergraduates who assisted me, Andres and Asa, thanks for the time and dedication. I hope that you have taken something away from this experience and continue your interest in research.

To Professor Hod Lipson, thank you for getting me interested in digital fabrication. I certainly would not have been able to come to MIT if it was not for you.

To David, Rehmi and all the other friends that I have met at the CBA, Media Lab and the rest of MIT, thank for your help getting through both the technical and emotional challenges of graduate student life. I hope I gave something back, too. I hope we can all stay in contact.

Most importantly to my family and Nadia, your love, support, and encouragement are the only reasons I have made it to the end of this program. Nadia, I literally could not have written this thesis without you. To Mama and Papa, thank you for always pushing me to do my best and instilling a love of learning in me since my earliest memories.

Contents

Abstract	2
Acknowledgments.....	5
Contents.....	6
Figures	8
Tables	10
1 Introduction	11
1.1 Motivation: biology’s manufacturing capabilities	11
1.2 Programmable matter by chain folding	12
1.3 Proposed approach: Stochastic actuation	13
1.3.1 Stochastic energy input	13
1.3.2 Smart clutches.....	14
1.3.3 Ratcheting.....	15
1.3.4 Continuum of controllability and complexity.....	15
1.4 Thesis overview	16
2 Background and previous work.....	18
2.1 Maxwell’s demon and the 2 nd Law of Thermodynamics	18
2.2 Rectified Brownian motion	19
2.2.1 Molecular biology	19
2.2.2 Micro-scale machines.....	19
2.2.3 Macro-scale machines	19
2.3 Chain programmable matter and robots.....	20
2.3.1 Moteins	23
2.4 Materials-based actuators.....	23
2.5 Clutch-controlled robots	25
2.5.1 Molecular clutches.....	26
3 Theory and scaling	28
3.1 Active chains in gravity.....	28

3.2	Passive chains.....	30
4	Design and construction of chain programable matter	32
4.1	Bimillimotein.....	32
4.1.1	Mechanical design	33
4.1.2	Electrical and control system	33
4.1.2.1	DC motor commutation sensing for position feedback.....	35
4.1.3	Results	38
4.2	Stochastic Moteins.....	38
4.2.1	Smart clutch system.....	39
4.2.1.1	Expected performance of smart clutch system	40
4.2.2	One-way bearing system	41
4.2.3	Single-position latching system	43
5	Ratchet performance studies.....	45
5.1	Description of simulation system.....	46
5.2	Description of mechanical system	48
5.3	Configuration.....	50
5.4	Length	51
5.5	Amplitude and frequency	53
6	Conclusion.....	55
6.1	Brownian rectification for programmable matter.....	55
6.2	Passive ratcheting chains.....	55
6.3	Future work.....	56
	References	57

Figures

Figure 1.1: Rendering of a dog constructed out of a continuous chain.....	12
Figure 1.2: A plot of a simulation of random torque applied to a joint and the response of its clutch. The red and green regions indicate when the clutch is closed and when it is open, respectively.....	14
Figure 1.3: Two different types of ratchet mechanisms: (left) a one-way bearing and (right) a ratchet and pawl.	15
Figure 1.4: Diagram illustrating a continuum of controllability and complexity in folding chain systems.....	16
Figure 2.1: Diagram illustrating Maxwell’s demon [5].....	18
Figure 2.2: Schematic diagram of Feynman-Smolchowski ratchet [11].....	20
Figure 2.3: a) Decomposition of a 2D pixel shape into sub pixels and then a traverse of those sub pixels by a continuous path b) A voxel-based 3D model that can be traversed by the same algorithm [2].	21
Figure 2.4: CAD rendering and photograph of a latching chain robot [12].	22
Figure 2.5: Photo and CAD rendering of the Millimotein [14].	23
Figure 2.6: a) Diagram of basic structure of a dielectric elastomer actuator [18] b) folded dielectric elastomer actuator allowing fabrication of large actuators from thin films [19].	24
Figure 2.7: Diagram and photograph of simple micro-hydraulic valve [14].	25
Figure 2.8: Diagram of single actuator with variable stiffness joints [21].	26
Figure 2.9: Photograph and rendering of solder clutch controlled crawling robot [22]. ...	26
Figure 2.10: Schematic representation of pentipycene-derived molecular clutch [23].	27
Figure 3.1: Illustration of forces involved in an active system lifting nodes in gravity. .	28
Figure 4.1: (Left) CAD model and (right) early prototype of the Bimillimotein.	33
Figure 4.2: CAD rendering of two connected Bimillimotein nodes. The rendering on the right includes a transparent node to indicate the location of the Hall effect sensor, motor, and circular array of alternating magnets.	34

Figure 4.3: LTSpice plot of DC motor commutation simulation. The blue line is current through the motor and the green line is voltage at one of the terminals. Spikes are generated by brush commutation..... 36

Figure 4.4: LTSpice model of DC motor commutation simulation..... 37

Figure 4.5: Photograph of one-way bearing stochastic Motein..... 42

Figure 4.6: Photograph and CAD rendering of cut-away view of single-position latching stochastic Motein. 44

Figure 5.1: Diagram illustrating stochastic folding experiment..... 46

Figure 5.2: Screen captures of a run of the folding simulation. The color indicates how far a node is from its target position..... 48

Figure 5.3: Photograph of the shake box set-up, highlighting the motor-driven actuation mechanism. 49

Figure 5.4: CAD models showing “cubic” fold geometry on left and “spiral” geometry on right. 50

Figure 5.5: Plot showing fold time versus fold geometry in experiment and simulation.50

Figure 5.6: Study of fold time versus number of joints folded. Each point represents a single experiment where an unfolded chain is agitated until it is completely folded. Simulated tests are in blue and experimental tests are in red..... 52

Figure 5.7: Ratchet increment size and chain length versus fraction of trials that succeed in simulation. 53

Figure 5.8: Plot showing folding time versus shake frequency and amplitude. Peak acceleration of the shaking motion is shown with contour lines. Note that time is in a logarithmic scale. 54

TABLES

Table 4.1: Comparison of Electromechanical Moteins.....	38
Table 5.1: Key parameters of the simulation	47

INTRODUCTION

1.1 Motivation: biology's manufacturing capabilities

Currently, almost all man-made manufacturing processes involve machines manipulating substrates that are smaller than and typically as precisely constructed as themselves, in a top-down fashion. In contrast, almost all manufacturing processes in biology are bottom-up. Such biological processes can manufacture systems with extremely high complexity at scales far below what is currently possible in artificial systems.

Even as some of the most advanced artificial manufacturing processes approach the complexity of biological systems, they lack many of the useful features of the latter, namely, self-reproduction, self-healing, and extreme adaptability in a system with relatively simple external inputs. Though these features are best exemplified by biology, they are not inherent to biology and can potentially exist in any system using self-assembly.

Self-reproduction is useful for the obvious goal of producing more of a desirable object without requiring any significant infrastructure other than the object itself. Self-reproduction also allows for evolution. In systems that cannot reproduce themselves entirely, minimizing the complexity and size of parts that cannot be self-reproduced can result in increased self-healing and adaptability. Such traits are useful in man-made systems operating in inaccessible or extreme environments such as in space exploration, search and rescue, or the battlefield.

1.2 Programmable matter by chain folding

If it is possible to create self-assembling systems that can be externally programmed to create desired shapes and even desired physical properties this would constitute programmable matter. In light of how well biology implements self-assembly and all of its positive characteristics, our research group is conducting a research program called “Millibiology” to create life in engineered materials [1].



Figure 1.1: Rendering of a dog constructed out of a continuous chain.

In Millibiology, our approach is to create arbitrary geometries through folding a continuous string onto itself in a similar fashion to protein folding [2]. Figure 1.1 illustrates how the shape of a dog can be constructed out of a single continuous chain of nodes. We are primarily exploring such systems with actuation built into each node.

The most obvious and reliable method for producing a self-folding chain is to implement actuators (such as motors) in each node. We call this a fully active system, as all the actuation is precisely controlled locally. Clearly, the benefit of such a system is that the chain should be able to fold reliably according to the implemented folding algorithm.

We have developed multiple iterations of fully active chains, though we quickly found that they are expensive and complicated to build and difficult to scale down. Such challenges prompted us to consider other approaches. Would it be possible to construct a system that is actuated through stochastic energy input externally, thereby removing the most complex element, the actuator?

1.3 Proposed approach: Stochastic actuation

In facing the challenges of developing a fully active system, we decided to develop an inherently different system that relies on external actuation (such as vibrating the entire system) and local control of clutches—which can be much simpler to implement, less expensive, and easier to scale down than actuators—to control node positions. In contrast to a fully active system, we call this proposed system a passive one. This is in some sense, a logical step in the context of Millibiology because this is of course how proteins are actuated to fold into their final configurations.

1.3.1 Stochastic energy input

There is a challenge in simply mimicking what proteins do. In water, at room temperature, a particle typically experiences over 10^{10} collisions per second [3]. Although these numbers are not typically reported in directed self-assembly research, observations of videos show that typical collision rates in these systems are in the 1–100 Hz range. Essentially, this is limited by the fact that the maximum speed of particles in these systems is either constant or decreasing as the objects scale up, while the distance the particles have to travel to the next object increases (see Section 3.2 for an analysis). This difference of many orders of magnitude significantly limits the rate of assembly.

One potential solution to this problem is to attempt to add longer range interactions to self-assembly systems [4]. This can effectively increase the rate of interactions, and also increase the success rate of interactions, but there are not always easy ways to implement this. Instead, we need another method to guide the system towards its goal.

While stochastic energy input can be applied to our system via vibrations to cause the chain to fold, there needs to be a way to control how the nodes move relative to each other. We propose the use of local clutches to achieve local control: 1) a smart clutch

that utilizes sensing to control when the clutch engages/disengages to control when motion occurs, and 2) an even simpler clutch, such as a ratcheted one-way bearing, which guarantees only a single locked end position.

1.3.2 Smart clutches

Probably the most sophisticated and powerful mechanism to use in this passive system is a clutch with some kind of torque or position sensing device to control the direction of motion and to even hold a joint in a fixed position. Figure 1.2 shows a plot from a simple simulation of joint angle over time in such a system for a single joint. The blue line indicates the random torque input, while the orange line indicates the angular position of the joint. In this simulation, the system is trying to reach the position labeled by the target line. Here, the state of the clutch is indicated by the color of the shaded vertical regions (green for open, red for closed).

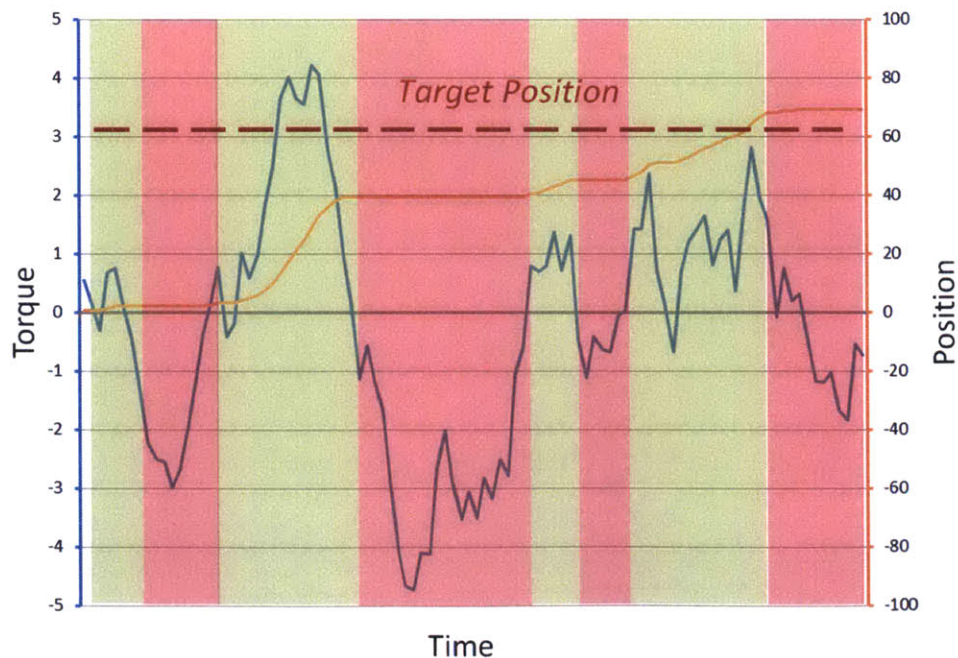


Figure 1.2: A plot of a simulation of random torque applied to a joint and the response of its clutch. The red and green regions indicate when the clutch is closed and when it is open, respectively.

1.3.3 Ratcheting

While a smart clutch would provide the ability to guide the system through arbitrary motion profiles and reprogram it in situ an even simpler system can be constructed by sacrificing these abilities.

In systems that have some kind of physical connection between units, as in the chain mechanisms we are studying, there is another option to increase the success rate of interactions, and that is ratcheting. Ratcheting is a mechanism that limits the motion of a system through configuration space by changing the potential landscape as the system moves through it.

Ratcheting can be implemented with mechanisms that are simpler than an actuator. Figure 1.3 shows examples of a passive mechanical ratchet as seen in a one-way bearing and a socket wrench. It is clear that both these mechanisms are purely mechanical and are simple to construct.

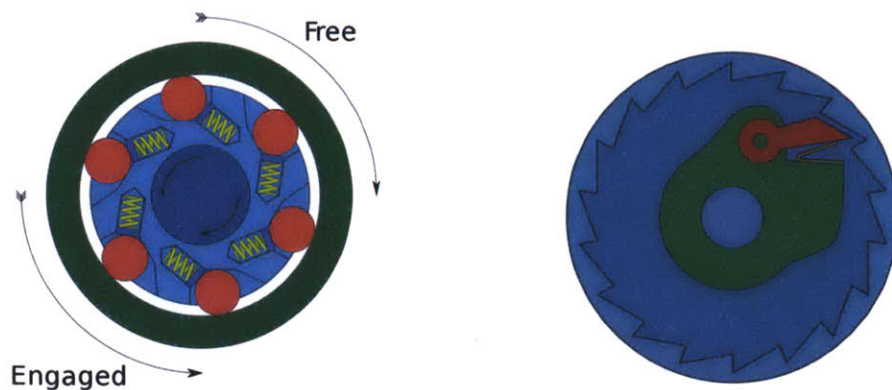


Figure 1.3: Two different types of ratchet mechanisms: (left) a one-way bearing and (right) a ratchet and pawl.

1.3.4 Continuum of controllability and complexity

Both a smart clutch and a purely passive ratcheting mechanism have advantages and disadvantages. The latter system is the most simple, but it is not programmable in situ, nor does it allow for programming of intermediate positions or paths through those

positions. Regardless, both of these systems are simpler to construct and have less control than a fully actuated system. Thus, a hierarchy (illustrated in Figure 1.4) emerges with increasing complexity allowing for increased control.

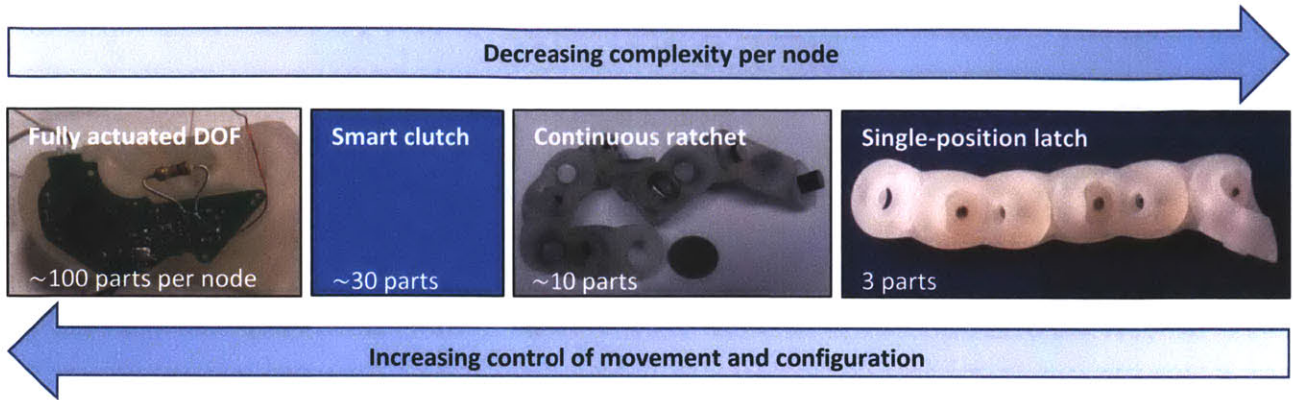


Figure 1.4: Diagram illustrating a continuum of controllability and complexity in folding chain systems.

1.4 Thesis overview

In Chapter 2, we introduce work from a range of fields including self-assembly, modular robotics, and rectified Brownian motion to help illustrate how our work is motivated by and relates to the state of the art.

In Chapter 3, we go through some basic analysis of how the physics of stochastically actuated chains scale with size.

In Chapter 4, we discuss the design of passive chain programmable matter systems and also present the design of a new active electromechanical system, the Bimillimotein, which is later compared to our passive systems.

In Chapter 5, we show the results of physical and simulated experiments of a passive ratcheting system to explore the effects of ratchet increment size and chain length as well as how the amplitude and frequency of agitation affect the folding time and success rate.

In Chapter 6, we summarize our results and suggest future directions for our work.

BACKGROUND AND PREVIOUS WORK

2.1 Maxwell's demon and the 2nd Law of Thermodynamics

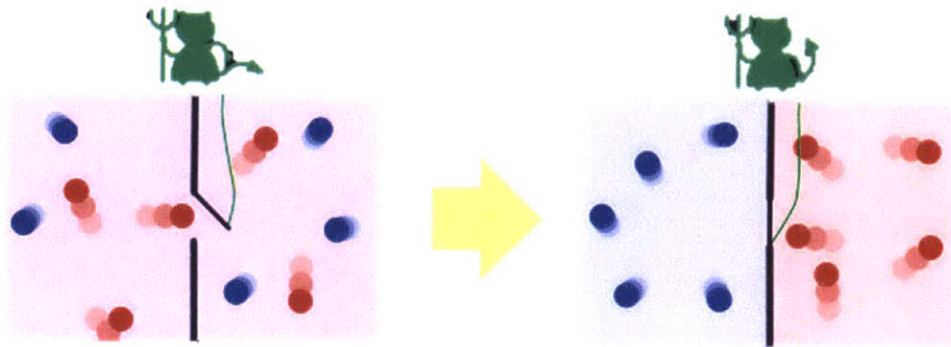


Figure 2.1: Diagram illustrating Maxwell's demon [5].

The system we are beginning to describe bears some resemblance to Maxwell's demon, and this may be of some concern to the reader. Maxwell's demon (illustrated in Figure 2.1) is a thought experiment in which a microscopic demon controlling a microscopic gate between two chambers opens the gate to allow high-temperature particles (red) to pass to one side and low-temperature particles (blue) to pass the other. This system seems to produce a temperature gradient without using any energy; the gate is very small and there is no obvious reason why it should take more energy to operate than is found in the particles. Of course, Maxwell's demon does not work in an equilibrium system, so what about the proposed system? Our system constructed at the macro-scale is not at equilibrium because the ratchet mechanism never becomes thermalized.

2.2 Rectified Brownian motion

2.2.1 Molecular biology

Rectified Brownian motion is a phenomenon behind many key biomolecular functions including a variety of transport mechanisms [6] [7] and potentially the action of myosin in muscle fiber [6]. For example, Ubiquinone is used to transport protons up an $8 \text{ k}_B\text{T}$ electric potential across a membrane, but the ATP that provides the energy for this does not act on the molecule directly; rather, it temporarily changes boundary conditions at the membrane and Brownian motion becomes the actual driving mechanism [6]. In general, it appears that rectified Brownian motion occurs so often in biology, that it is used as a mechanism that allows for complex or long range motions in a relatively simple fashion. This seems related to our idea to use it to reduce the complexity of our Motein units.

2.2.2 Micro-scale machines

At the micro-scale, researchers have implemented Brownian ratchets that can cause particles to diffuse preferentially in one direction by pulsing an anisotropic electric field [8]. Though the electric field contributes to the forward motion, there is no commutation or coordination with the motion of the particle. The field can be thought of as simply reinforcing Brownian motion preferentially in one direction. These systems have been successfully employed to manipulate small particles and to construct filters.

2.2.3 Macro-scale machines

At the macro scale, there have been experiments into implementing a so called Feynman-Smolchowski ratchet. A Feynman-Smolchowski ratchet couples a microscale ratchet to a paddle wheel in a heat bath, as in Figure 2.2. The motion of the particles applies random forces to the paddle T1, but the ratchet T2 only allows motion in one

direction. A load can be applied to the shaft, thereby extracting work. This might seem to be a working Maxwell’s demon, but as Feynman showed, it fails in equilibrium systems because the ratchet would vibrate and fail to prevent backward motion at the precise rate that it achieves forward motion [9]. In the macro-scale constructions of the Feynman-Smolchowski ratchet, researchers simulated a thermal bath with an aggressively vibrated chamber filled with metal ball bearings and a one-way bearing for the ratchet portion. As the researchers note, this heat bath is out of equilibrium with the ratchet mechanism and the bath itself is not in thermal equilibrium as the interaction of it and the paddle wheel develops a convective current that reinforces the motion [10]. Nevertheless, this demonstrates the basic concept at the core of this thesis: rectifying random motion is a means to move the actuator out of one part of the system.

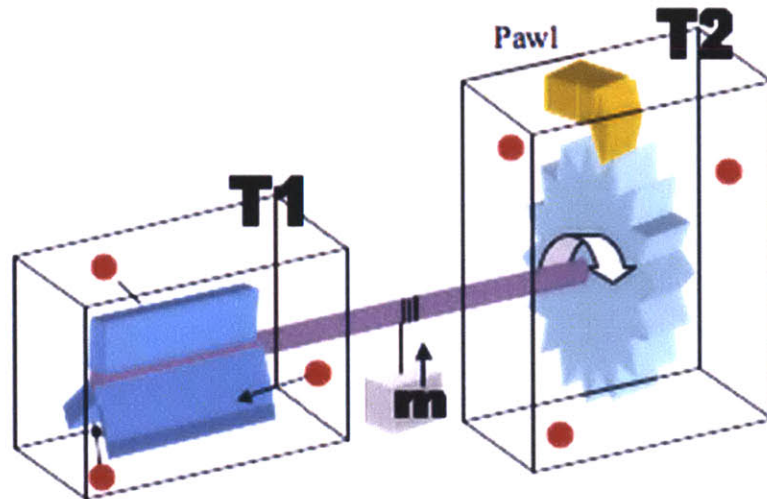


Figure 2.2: Schematic diagram of Feynman-Smolchowski ratchet [11].

2.3 Chain programmable matter and robots

One way to implement programmable matter is to use modules connected in a chain architecture. By providing a permanent connection for transferring power and information between nodes while also allowing significant flexibility close to that of

systems with non-connected nodes, this removes some of the difficulties often found in a system with separate modules. Most early embodiments of this concept rely on many small robotic modules that have mechanisms for detaching/attaching to each other and self-manipulating [12] [13]. Requiring such capabilities typically adds bulk and reduces the performance of the finished object. One way to avoid such losses is to use a continuous chain of modules as the basic structure.

However, the chain structure introduces a new challenge. Now that the modules are not arbitrarily reconfigurable, how does the system produce arbitrary configurations? In our research, we have found a universal folding algorithm that can take any voxelized 3D shape and find the necessary folds to make a chain fill that shape. Additionally, we have built simulation environments capable of finding physically possible motion profiles to fold one of these chain robots into a given shape [2]. Figure 2.3 provides an example of an algorithm used to find a continuous folding path in two dimensions.

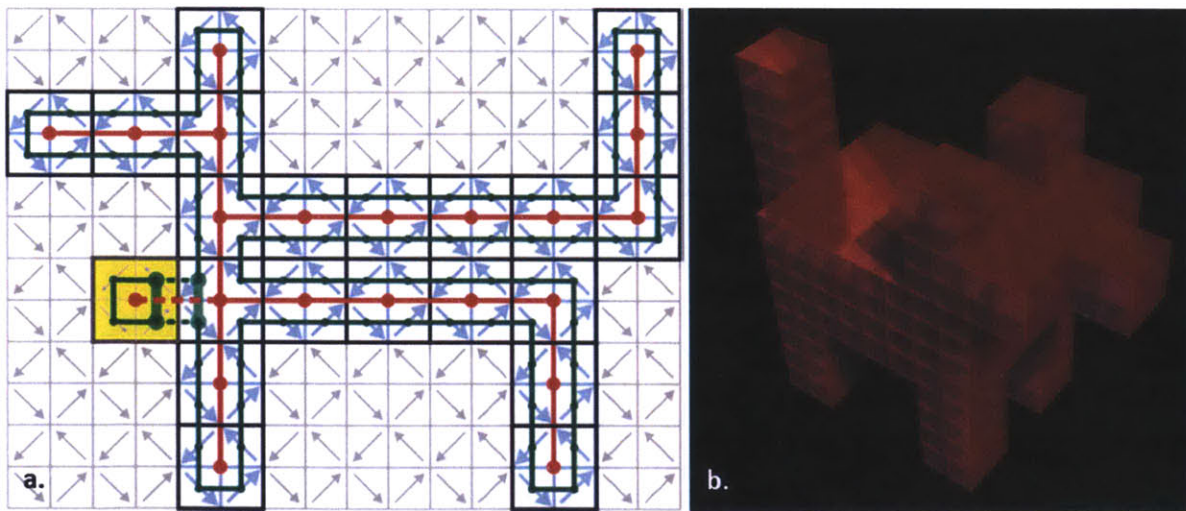


Figure 2.3: a) Decomposition of a 2D pixel shape into sub pixels and then a traverse of those sub pixels by a continuous path b) A voxel-based 3D model that can be traversed by the same algorithm [2].

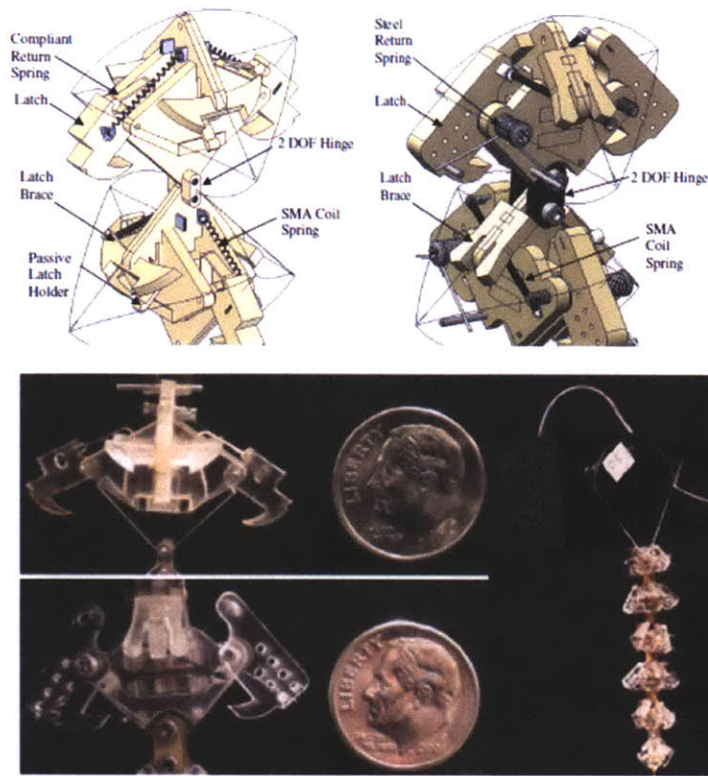


Figure 2.4: CAD rendering and photograph of a latching chain robot [12].

Another direction that researchers are pursuing is to remove the actuator in each node and, instead, have a single actuated joint at the end of the chain to fold the chain while each joint latches in position [12]. This is shown in Figure 2.4. This obviously bears great similarity to the concept pursued in this thesis. The important difference is that we implement the energy input stochastically without a specific dedicated structure. This allows our system to potentially use different actuation sources, or scavenge energy from the environment.

2.3.1 Moteins

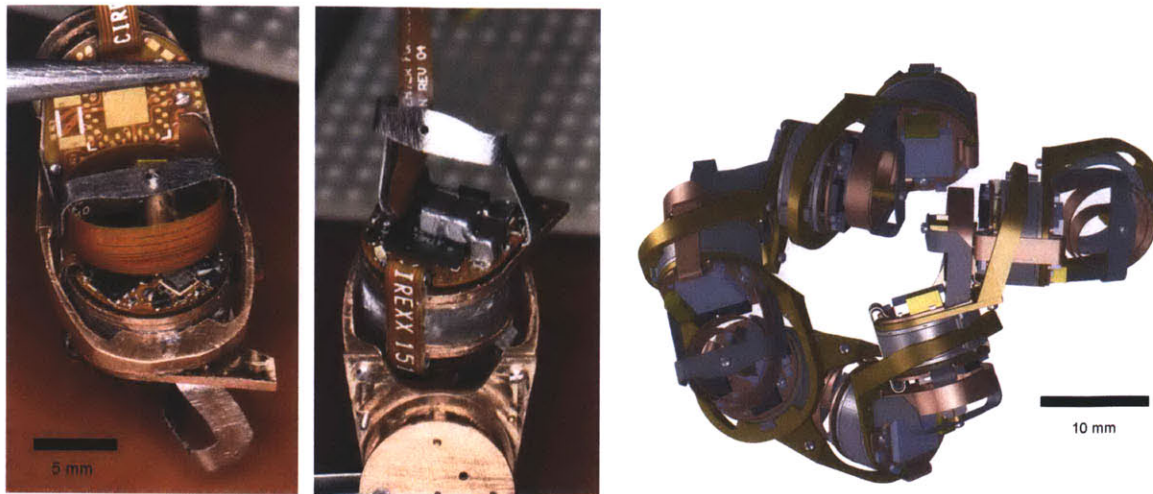


Figure 2.5: Photo and CAD rendering of the Millimotein [14].

Under the Millibiology program, the MIT Center for Bits and Atoms has designed and built several versions of active, electromechanical chain programmable matter. These devices all shared the same geometry based on hexagonally bisected cubes, which is also the same geometry used in the Molecubes project [13]. In comparison to other universal folding geometries such as the right-angle hinged tetrahedron [15] this geometry allows for a large volume inside each joint to place an actuator. Though there have been several versions, the most developed by far has been the Millimotein [14]. The goal of this project was to construct a system with nodes 10mm in diameter. This is a significant feat because the system requires a high torque motor, bearings, and electronic control in each node. This system uses a new type of motor called an electropermanent motor in a wobble motor configuration, providing very high torque and a gearing effect without the complexity of additional shafts or gears.

2.4 Materials-based actuators

Materials-based actuators fit naturally with the smart clutch concept, as they provide a simple mechanism for implementing the clutch actuator while keeping the complexity

low. Because the clutch does not require as high force or power as an equivalent fully active system, the limited performance of materials-based actuators may be adequate here when they have failed in more traditional robotics applications.

There has been recent progress in materials-based actuators and their application to robotics. One group is already demonstrating the advantages of materials-based actuators by building a self-folding sheet that, because of its thinness, can only utilize such actuators [16].

There are many instances of materials-based actuators in the literature, but we have identified three that are of interest because they have already shown performance sufficient for this application [17]. We also believe that these technologies have future potential for other applications and are worth developing: dielectric elastomers, electrolytic gas generation, and micro-valving with a conventional pressure source.

Dielectric elastomer actuators are interesting because across all parameters, they meet or surpass the capabilities of mammalian muscle. They are also potentially adaptable to many different configurations mimicking those found in natural muscle.

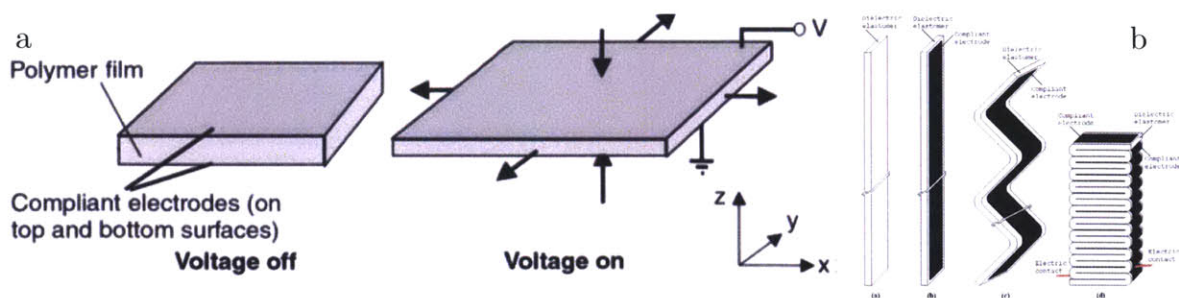


Figure 2.6: a) Diagram of basic structure of a dielectric elastomer actuator [18] b) folded dielectric elastomer actuator allowing fabrication of large actuators from thin films [19].

Electrolytic gas generation is promising because it has the potential for high forces and strains with low actuation voltage [20]. One major drawback is the slow speed, which is

an important consideration for this application because the clutch should be able to switch its state relatively rapidly.

Fluidic actuators at larger scales are capable of very high power/energy/force densities, high strains and speeds, and relatively simple control. However, as we miniaturize them one of the key limiting factors is miniaturizing the valve. The actuator can be kept relatively simple by using a balloon or bellows architecture, but the valve typically requires precision moving parts. Figure 2.7 illustrates a potential design for a micro-hydraulic valve that is very simple. It simply requires a pipe with a special internal shape, a ferromagnetic ball, and an electromagnet or electropermanent magnet. By using relatively soft materials for the pipe, the precision requirements to achieve sealing can be reduced.

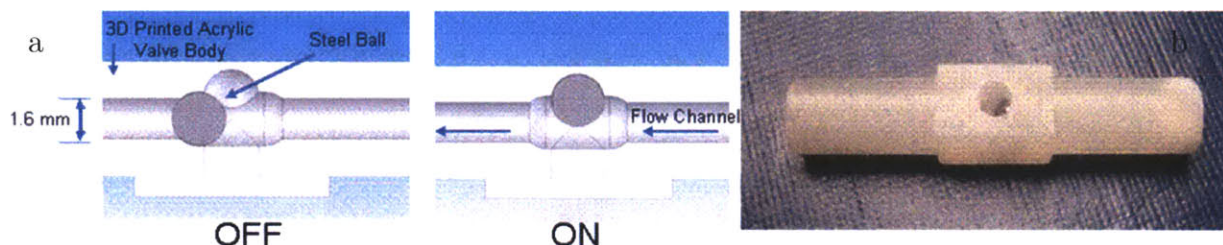


Figure 2.7: Diagram and photograph of simple micro-hydraulic valve [14].

2.5 Clutch-controlled robots

Robotics researchers have also been exploring the use of clutches in simplifying their machines by reducing the number of actuators required. These systems can have effective degrees of freedom up to the number of clutches multiplied by the number of actuators.

One instance of this system has the clutch mechanism at every joint. A single set of actuators at the base of a serial kinematic chain of lockable joints can act as if there were actuators at every clutch as shown in Figure 2.8.

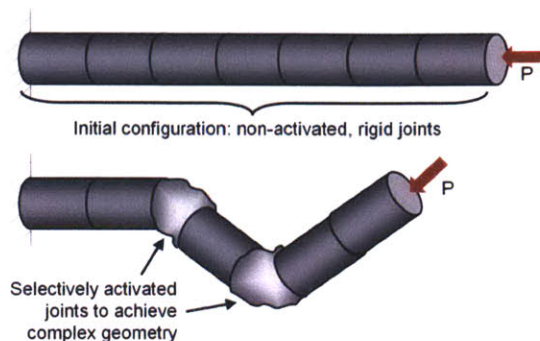


Figure 2.8: Diagram of single actuator with variable stiffness joints [21].

In a variation of this system, a parallel kinematic mechanism with three locking joints and a single actuator can provide three degrees of freedom

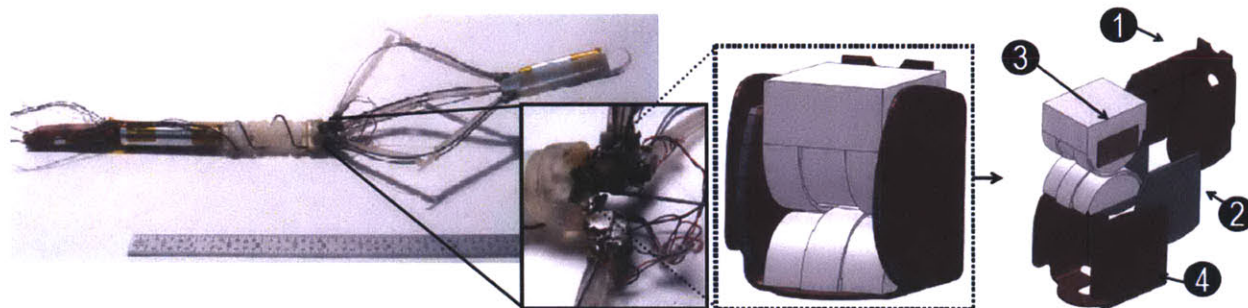


Figure 2.9: Photograph and rendering of solder clutch controlled crawling robot [22].

2.5.1 Molecular clutches

Clutches are useful for miniaturizing robotics, but how small can they be made? Researchers have demonstrated a range of MEMS mechanisms that can be used as clutches, but at the extreme small end of miniaturization, chemists have constructed molecules that behave as clutches. These molecules have a moiety that is free to spin in one state but not in the other state [23]. They can be switched from one state to the other by simply being illuminated with a particular wavelength of light as shown in

Figure 2.10. Potentially, this moiety could be bonded to other structures to incorporate the molecule into a larger system. A more serious issue would be to address individual clutches in a system.

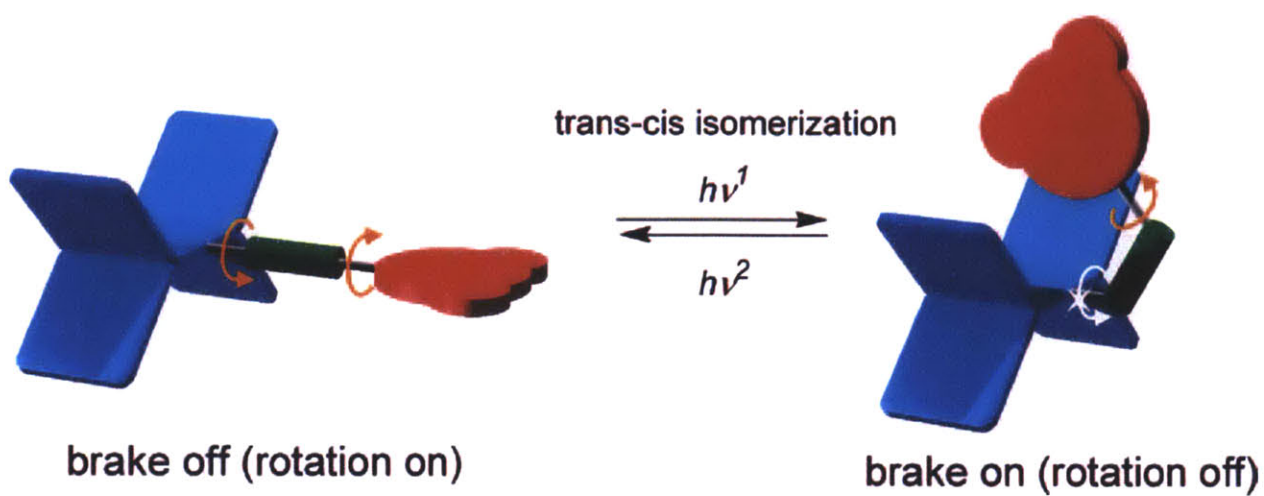


Figure 2.10: Schematic representation of pentipycene-derived molecular clutch [23].

THEORY AND SCALING

3.1 Active chains in gravity

One of the key parameters that determines the functionality or usefulness of chain programmable matter is the number of nodes—in a fully stretched out configuration—a single node can lift in gravity. This is known as the “arm wrestling number” for the system. Figure 3.1 illustrates this concept.

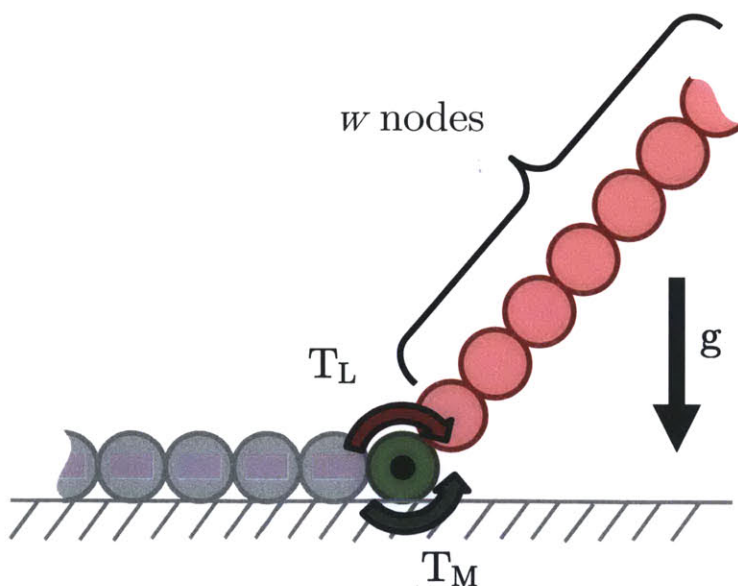


Figure 3.1: Illustration of forces involved in an active system lifting nodes in gravity.

The arm wrestling number indicates how mobile and active a chain robot can be. Under the influence of gravity, the space of all possible motions is limited by the requirement that moving nodes need to be able to lift their neighbors through gravity. To ensure successful folding, a chain of n nodes needs an arm wrestling number of

approximately $n/2$ (half the chain on the ground and half being lifted in the air). However, much smaller ratios of arm wrestling number to chain length can probably yield useful amounts of mobility. This is especially true because an arch formed in the middle of a chain is lifted from both ends, so the arch could be approximately twice as long as the arm wrestling number. Additionally, if gravity is taken into consideration, motion profiles can be slightly reconfigured to make large motions occur perpendicular to gravity, or eliminated altogether.

While examining the utility of programmable matter for a wide range of applications, it is useful to understand how a given system's arm wrestling number would change as the design is scaled up or down. The following is an analysis of this:

We will use r to represent the size of the design. The motor has a gap with magnetic field that applies a torque on the shaft. The field applies a force proportional to the area of a gap, r^2 , that then creates a torque proportional to the distance of the gap from the center of the motor, r . Therefore, for a given motor design, the motor has a maximum torque T_M proportional to r^3 . This agrees with the analysis in [14].

Note that while we are specifically discussing electrical motors here, this analysis yields the same basic relationship for other types of actuators including hydraulics and a variety of materials-based actuators.

The torque applied by the load on the motor, T_L , is the sum of the torques caused by the weight of all the other nodes under gravity

$$T_L = \sum_{i=1}^w d_i m g \tag{3.1}$$

where d is the distance of the node to the rotating node, m is the mass of a node, g is acceleration due to gravity. Rewriting in closed form and with $l = wr$ and with m proportional to r^3 .

$$T_L \propto n^2 r^4 \tag{3.2}$$

Setting $T_L = T_M$ and solving for w

$$w = \sqrt{\frac{1}{r}} \tag{3.3}$$

So, the number of nodes that can be lifted against gravity increases as the size of the nodes decrease. This is as expected as insects are known to be able to lift many times their own weight, while the largest mammals cannot even support their own weight and must live in buoyant environments.

In terms of the length of the chain of nodes being lifted, by multiplying both sides by r , the relationship becomes

$$l \propto \sqrt{r} \tag{3.4}$$

This also matches our intuition in that larger machines can move longer, unsupported loads.

3.2 Passive chains

As we mentioned in the introduction (Section 1.3.1), one of the issues with self-assembly processes at larger scales is that the rate of interactions, and thus the rate of assembly seems to go down as the scale increases. Here, we present a simple analysis explaining why this is true for our system.

To start with, we must understand why we cannot simply increase the rate of shaking to increase the rate of folding. This is because there is a critical speed at which the structures in the system will not be able to survive the impacts during folding. In a chemical system, this corresponds to increasing temperature to increase the rate of reaction until the temperature is so high that the product or reagents begin to break down.

Assuming a completely inelastic collision, all of this energy must be absorbed by a node or joint. For a given design, the amount of energy a part of the structure can absorb in an impact is proportional to its volume. Therefore the shaking energy, E_s , that joints can sustain is proportional to the volume or r^3 :

$$E_s \propto r^3 \tag{3.5}$$

With the inelastic collision assumption, the energy a node has to absorb is the kinetic energy in another node:

$$E_s = \frac{1}{2}mv^2 \tag{3.6}$$

With $m \propto r^3$, we get

$$E_s \propto \frac{1}{2}r^3v^2 \tag{3.7}$$

For both (3.5) and (3.7) to be true, v must remain constant at any scale.

The distance a node is required to move to fold is inversely proportional to v , which is constant, and proportional to the distance to travel. Hence,

$$t \propto r \tag{3.8}$$

Therefore, the folding rate increases as the system is scaled down. The analysis in the previous section regarding gravity can be applied here to analyze the peak acceleration (applied by vibrations). This peak acceleration, or the length of chain that can sustain a given acceleration, also increases as the chain is scaled down.

Overall, this means that these systems are more “interesting” in that they can fold more complex systems at smaller scale. Additionally, with our current fabrication methods, as systems are scaled up, cost becomes more dependent on raw material costs than costs due to complexity. This reduces the advantage of using passive systems.

DESIGN AND CONSTRUCTION OF CHAIN PROGRAMMABLE MATTER

4.1 Bimillimotein

To examine our new passive Moteins in relation to active electromechanical systems, we needed a suitable system to compare to. The various existing Motein systems have all been built with goals in addition to the goal of building an effective active Motein system. In some cases, our systems were exploring very large Moteins, or novel actuators, but none have been designed solely with the goals of improving performance (speed, torque, and number of nodes) and reducing cost and complexity. Therefore, we decided to design a new chain with these goals in mind.

One of the key parameters that affects the size of the largest structures a Motein can fold is the arm wrestling number. As indicated in Chapter 3, this number increases for a given design as the design is scaled down. This means that we want the new design to be as small as possible. At the same time, to reduce cost and complexity we should use commercial-off-the-shelf components as much as possible. For our electromechanical systems, this eventually led to setting the size of the system based on the smallest easily available DC gearmotors. The name “Bimillimotein” refers to the fact that it is twice the size of the Millimotein which is the core platform of the Millibiology project.

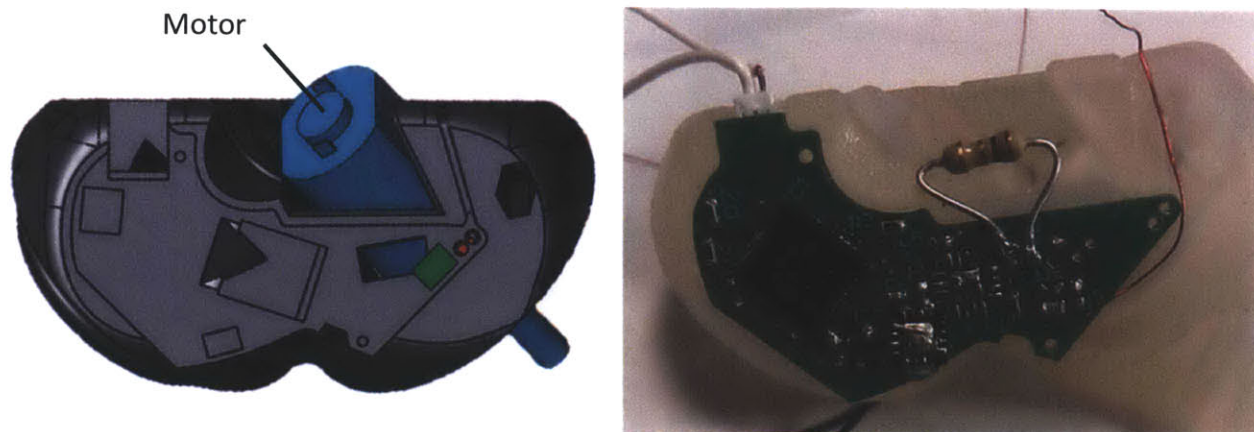


Figure 4.1: (Left) CAD model and (right) early prototype of the Bimillimotein.

4.1.1 Mechanical design

The overall scale was determined by setting the smallest DC gearmotors with relatively high reduction ratio ($\sim 100s:1$). A 298:1 ratio metal gear motor was chosen and a shell was designed to fit around it. Before continuing with the design, we constructed a number of nodes only populated with motors to test the arm wrestling number of the system. We found that this system was capable of an arm wrestling number of 7-8 without excessively heating the motor.

The shell was designed to be taken apart with two screws and the motor simply slid into the shell. This allowed easy assembly and disassembly.

4.1.2 Electrical and control system

The Bimillimotein electronics system needed to provide communication along the chain and closed-loop control of joint position. The other primary goal driving the design was to miniaturize the system, reduce cost, and reduce complexity of assembly and integration into the mechanical system.

The list of key features in the system is below:

- I2C bus for node to node communication

- RGB led for visual feedback
- H-bridge for speed and direction control of motor
- Current sensing and voltage sensing for motor H-bridge
- Custom analog Hall effect position sensing system

We explored many options for the position sensing system but did not find any complete system (potentiometer, optical encoder, magnetic encoder, etc.) that fit the small size requirements and the requirement that the device not be coaxial with the axis of rotation (because the motor takes that position). As a result, we devised a system of alternating polar magnets and a small, Hall Effect positioning system with integrated signal conditioning to perform the sensing. This system is shown in Figure 4.2.

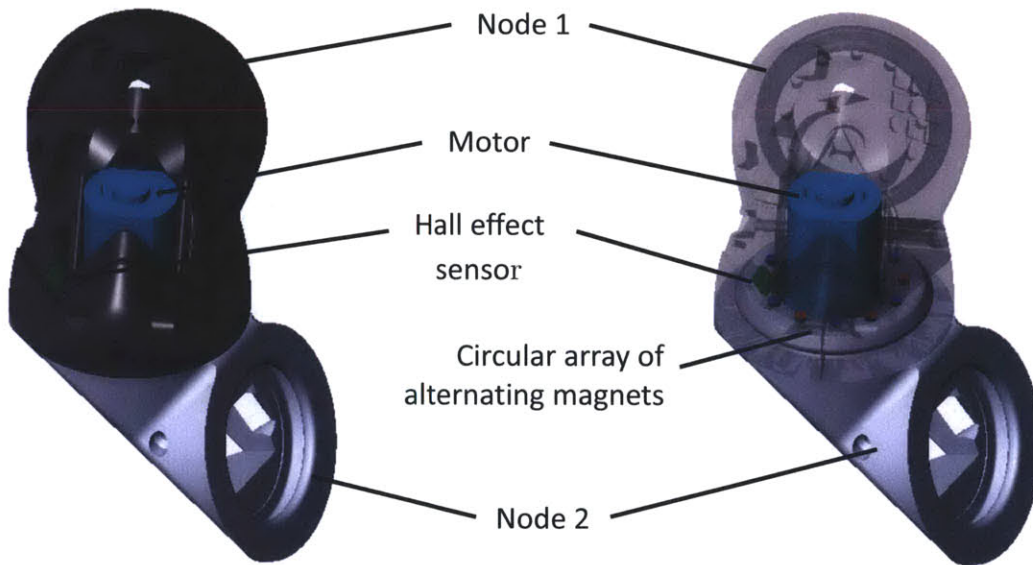


Figure 4.2: CAD rendering of two connected Bimillimotein nodes. The rendering on the right includes a transparent node to indicate the location of the Hall Effect sensor, motor, and circular array of alternating magnets.

In principal, using the analog signal from the Hall Effect sensor should have allowed accurately sensing within ~ 100 intermediate positions per magnet, but this turned out to be difficult to realize. Because of variations in fabrication of the magnets, and in

their positioning within the assembly, the signal from each magnet varied by $\pm 10\%$. This significantly reduced the ability to use analog interpolation. One way to get around this problem is by calibrating each node after installation of the magnets by rotating through the entire range of motion. Instead, we chose simply to adjust the hard-coded parameters to work with the entire range of magnet values. This reduced the worst-case accuracy and resolution to ~ 10 intermediate positions per magnet (~ 120 per revolution), which was sufficient for this application.

4.1.2.1 DC motor commutation sensing for position feedback

In early stages of the system design, we investigated position sensing based purely off sensing commutation of brushes in the DC motor and knowledge of voltage and current input into the motor. This would constitute a minimally complex and bulky sensing solution. Though this method was not used in this system, we document it here for future applications.

In general this technique is referred to as ripple counting and is a known technique for sensing the motion of DC brushed motors [24]. However, this technique does not appear to be used for determining absolute position determination in robotics applications.

Through a combination of simulation and experimentation we tested circuit topologies and algorithms to try to combine this technique with motor voltage and current sensing to reliably determine absolute angle.

Figure 4.3 shows a plot generated by an LTSpice simulation of the circuit shown in Figure 4.4. The spikes are pulses during which a brush breaks contact during commutation so the speed of the motor is the inversely proportional to the distance between spikes. An important feature of this system is that the Spice model simulates the coupled electrical and mechanical aspects of the motor. In simulation, a load can be

applied to the motor. For example, the plot shows the motor spinning up to speed with an inertial load and friction applied to it creating the characteristic, asymptotic ramp up in speed.

The simulation accurately modeled most of the phenomenon exhibited in the real system, and we were able to get the real system to track position reasonably well under most conditions except when the motor was travelling at very slow speed.

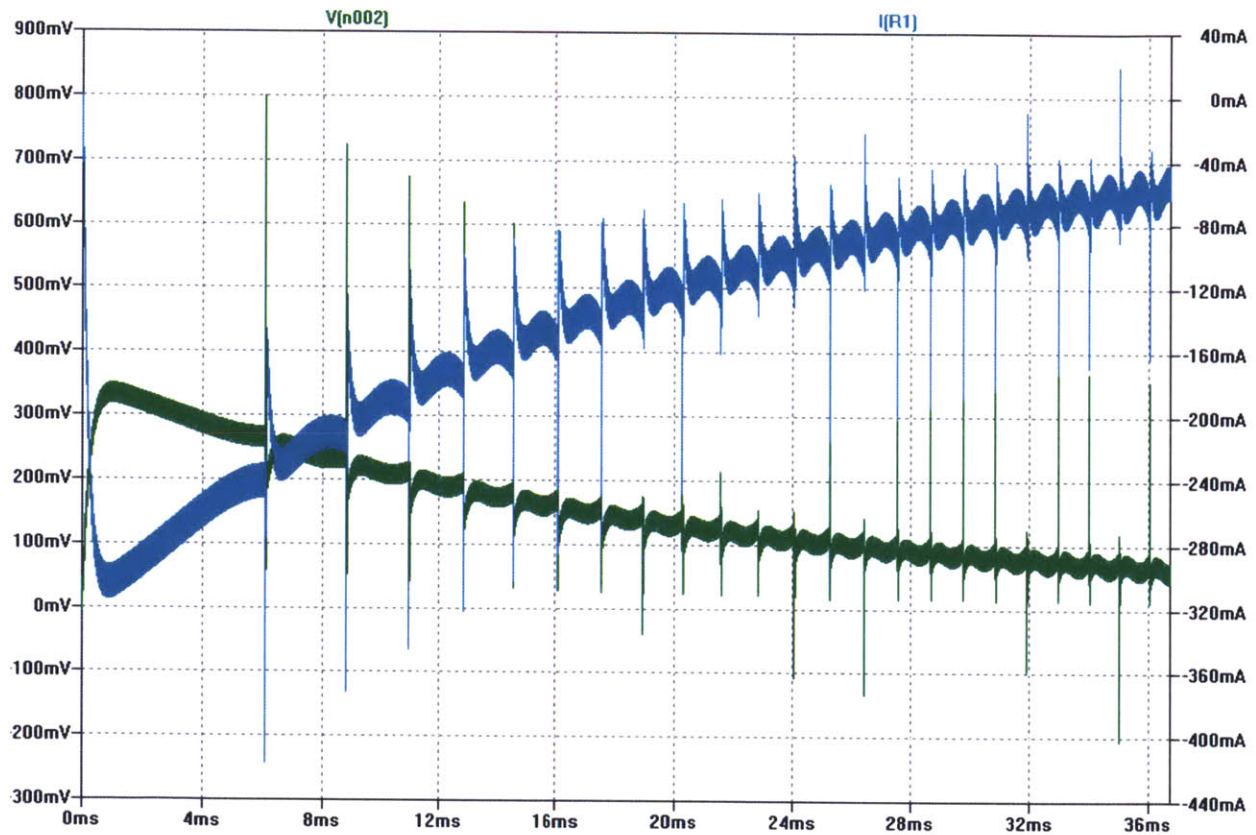


Figure 4.3: LTSpice plot of DC motor commutation simulation. The blue line is current through the motor and the green line is voltage at one of the terminals. Spikes are generated by brush commutation.

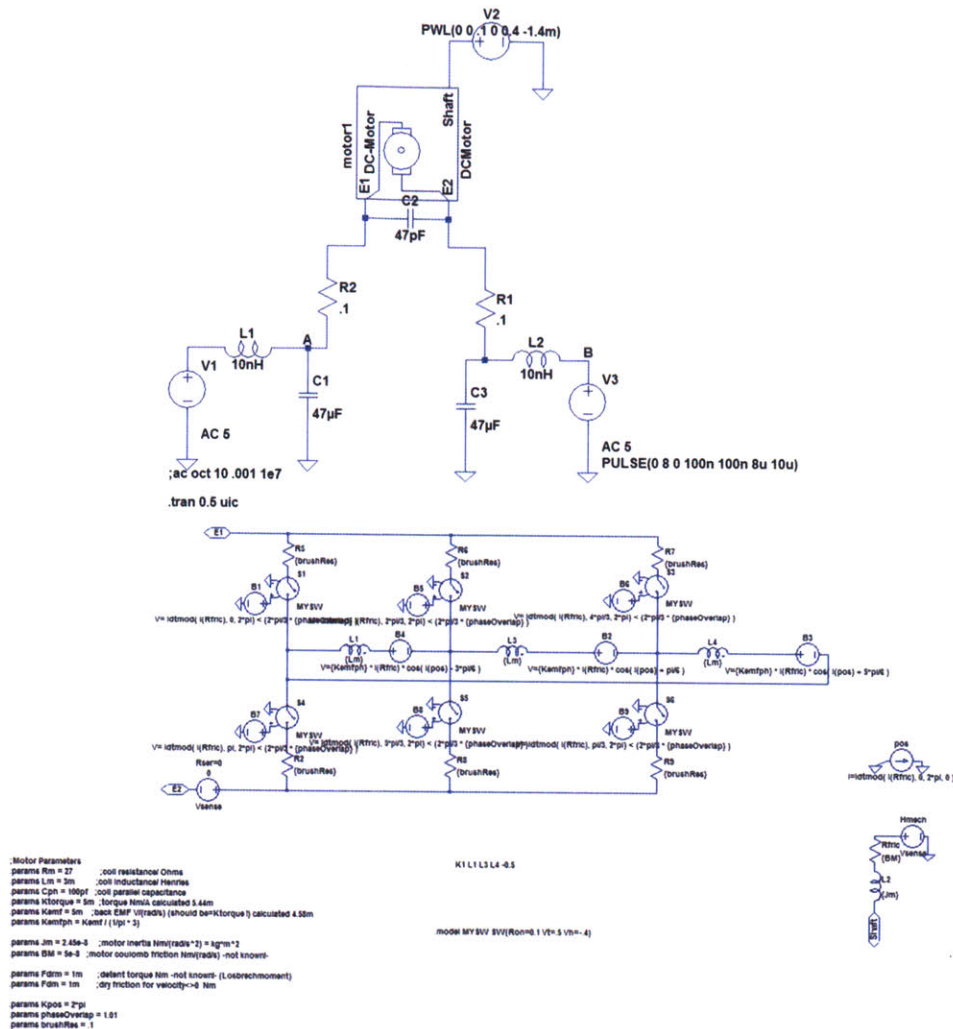


Figure 4.4: LTSpice model of DC motor commutation simulation.

One technique that was not investigated for determining the direction of motion is to use the asymmetrical windings of coils found in many brushed DC motors. The asymmetrical winding varies the inductance depending on the direction that the motor is moving in, which could be detected by monitoring the voltage and current at the motor terminals and combining that with speed information. However, this signal may also be difficult to detect at low speeds.

4.1.3 Results

The Bimillimotein design met the goals of significantly increasing the arm wrestling number. Additionally, it greatly improved the maximum speed achieved compared to other Moteins. Table 4.1 lists all of the Moteins built to date with arm wrestling numbers, arm wrestling numbers scaled to a 12mm system (according to the rule given in Section 3.1), and maximum angular speed. Though the normalized arm wrestling number should not solely be used to compare different designs, one should note that much of the difference comes from the difficulty of employing large gear ratios at small sizes. To account for this, a useful metric might be the scaled arm wrestling number multiplied by the maximum angular speed.

Table 4.1: Comparison of Electromechanical Moteins

System size (mm)	Arm wrestling number		Max speed (rpm)
	Arm wrestling number	scaled to 12 mm system	
Skylar (450)	2	12.2	~1
Kenny (76)	4	10.1	17
Max (24)	7	9.9	80
Ara (12)	1	1	~1

4.2 Stochastic Moteins

Though the bimillimotein design did meet many of our goals of increasing agility and decreasing complexity when compared with earlier active Motein systems, it was still too complex to achieve very long chains. Therefore, we continued to investigate more passive systems to attempt to find an appropriate balance.

4.2.1 Smart clutch system

Although we did not implement the smart clutch system, we did consider how it could be done. In particular, there are some interesting choices for implementing its sensing and control system.

To review, this system functions by selectively applying a clutch to each node. The system should open the clutch when the torque on the node is towards a desired target and should close the clutch when the torque is away from the target. One way to accomplish this is to directly monitor the torque with an appropriately placed strain sensor or something similar. This system would also need some sort of position sensor to determine which side of the target position the node is at. This could be a relatively simple two-position sensor. However, if a high resolution sensor is implemented there is another option for torque sensing.

If the system already has a high resolution position sensor, it may be possible to do away with the torque sensor. In this scheme, a sort of instantaneous torque measurement is made simply by opening the clutch, measuring which way the joint is moving in, and then either closing or leaving the clutch open based on this information. How well this system would work would depend crucially on the bandwidth of the position sensing system, the bandwidth of the clutch, and the spectrum or characteristics of the random energy input. If the clutch cannot respond fast enough or the position sensor cannot sense quickly enough, ground would be lost during these sampling periods, or the system could overshoot the target.

In addition to the node position control system, the smart clutch system presents interesting challenges in higher-level coordinated control of all of the nodes in the chain and path planning. Finding motion profiles for active Motein systems of significant length and that do not intersect is already a challenge being explored by other

researchers [25]. The smart clutch system adds an additional challenge, because the more precisely the system attempts to execute a profile, the longer it would take. Because of the randomness of the motion, it can take arbitrarily long to reach a target position, and the more positions that are added (in time and number of nodes) the worse this problem becomes. Therefore it is desirable to specify the motion profile as an envelope of motion profiles, or a motion profile with tolerances to allow the system to fold faster. Calculating such a profile is a new, difficult problem for researchers interested in the algorithms of this problem to tackle.

4.2.1.1 Expected performance of smart clutch system

Even without constructing a smart clutch system, we can estimate its performance from a few calculations. For this analysis, we chose to design a system of size comparable to the Millimotein as it would be ideal to use the advantages of the smart clutch system to construct a small system. We also chose to evaluate an electropermanent magnet based clutch, as the design and performance of these technologies are relatively well understood. The design would look similar to the Millimotein except that the complex stator portion of the motor would be replaced by a single large electropermanent magnet, simplifying its construction. The electronics would also be simplified as there would only be a single phase to drive.

The key performance metrics to understand are the torque that the clutch can sustain, and the bandwidth of the clutch. Based on high speed video of the Millimotein, these electropermanent magnets can actuate and close a gap in approximately ~ 2 ms. This gives a bandwidth of approximately 250 Hz. This should be sufficient to control the system effectively under the ~ 10 Hz vibrations that we would apply to it.

The torque the clutch can sustain can be calculated from the pressure the electropermanent magnet can exert and its area. Using a magnet pressure of 1 MPa, a

coefficient of friction of 1, area of magnet of 30 mm^2 and a lever arm of 4 mm (all comparable to the Millimotein design), we get a clutch torque of 40 mNm. This compares to the measured torque of the Millimotein motor of $\sim 1.1 \text{ mNm}$ [14].

To understand how long of a chain this clutch could handle being agitated with without slipping is a more difficult question. One simplistic answer is to do an analysis similar to the arm wrestling number analysis in Section 3.1 but with a higher value for the acceleration due to gravity. Using an acceleration due to gravity of 30 ms^{-2} , node mass of 5 g, and node pitch of 12 mm, we calculate an arm wrestling number of approximately 6.5 as compared to the Millimotein's 1.5. Finally, based on the results of Chapter 5, we can expect folding times on the order of 10s of seconds. This is comparable to the Millimotein.

4.2.2 One-way bearing system

The smart clutch system presents a number of new design and fabrication challenges. A sensible first step to get to a working smart clutch system is to start with the passive ratcheting systems. This will help us better understand what it takes to build systems robust enough to survive the agitation, and learn more about the bandwidth requirements of its sensors and actuators.

The first physical implementation of the passive ratchet concept was a chain using the typical Motein/Molecube geometry with a locking roller type one-way bearing similar to the one shown in Figure 1.3. Each node is composed of a few key parts:

1. The shell was printed on a 3D Systems Invision 3D printer
2. A 10 mm ceramic coated aluminum shaft pressed into the shell
3. A 10 mm internal diameter deep groove radial ball bearing pressed into the shell
4. A 10 mm internal diameter one-way bearing of a type often used in fishing reels



Figure 4.5: Photograph of one-way bearing stochastic Motein.

When a chain of this one-way bearing system was placed in a box and shaken lightly by hand, it quickly (a few seconds) folded itself into the programmed shape. Because the one-way bearings had zero visible backlash, and the ball bearings provided very free rotation, it took very little acceleration to cause each joint to make progress. Reprogramming was performed by removing each one-way bearing and installing it in the reverse direction.

Though there are relatively few parts in this system, assembly, reprogramming, and repair of chains proved difficult because all of the parts were press-fit into the brittle 3D printed acrylic material which was susceptible to breaking. Additionally, the system was not robust enough for repeated use and would begin to fall apart after a few cycles. One of the reasons for this was the significant weight of each node because of the large amount of metal in each part.

4.2.3 Single-position latching system

We believe it would have been possible to create a more robust system based on one-way bearings, but because of a desire to explore even simpler systems, we pursued a single-position latching system. The basic design we came up with, shown in Figure 4.6, had the following parts:

1. Shell printed on a 3D Systems Invision 3D printer. These came in left and right folding variations.
2. A small cap piece called the “mushroom” with a molded-in threaded insert installed. Also 3D printed.
3. A screw to hold these parts together

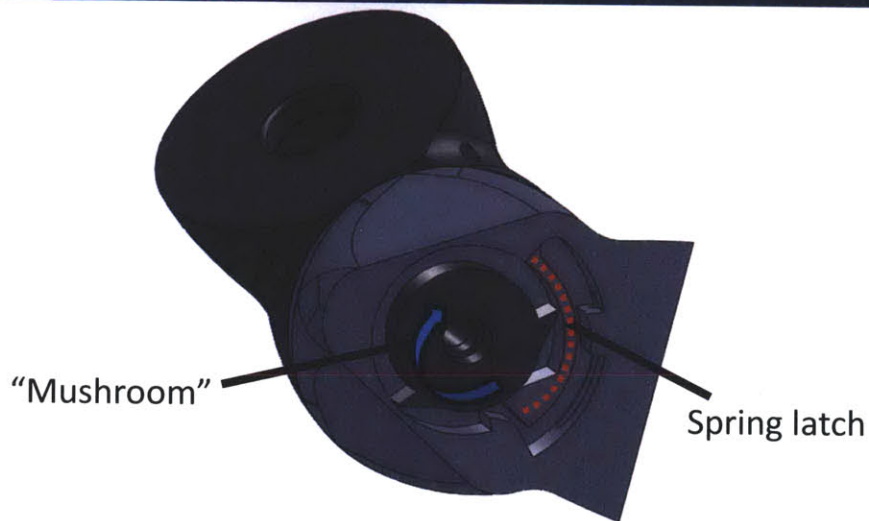


Figure 4.6: Photograph and CAD rendering of cut-away view of single-position latching stochastic Motein.

After a few revisions of the design to tune the latch mechanism, the device was repeatable and reliable and each unit could survive many (10s) tests and resets.

RATCHET PERFORMANCE STUDIES

Now that we understand the need for stochastic programmable matter and a few potential instantiations of the design, we can explore how such a system performs. Figure 1.2 shows a simple simulation of a random torque applied to a joint. The joint senses this torque and opens and closes its clutch to try to ratchet the joint towards the desired to angle (dashed line). When the clutch is open, the background is green, and when the clutch is closed, the background is red. This plot is useful in illustrating two things: 1) the importance of sensor and clutch bandwidth and input noise spectrum in determining how fast and efficiently the joint can move. 2) The fact that motion profiles across many joints cannot be precisely specified over time because the time to reach a target position is unknown. These two questions are at the center of this thesis.

The basic experiment that we conducted was to agitate an un-folded chain until it successfully folded into its desired position, and to measure the amount of time that this operation took. This is illustrated in Figure 5.1. This chapter first describes the simulation and experimental systems used to study these parameters and then delves into examining the data.

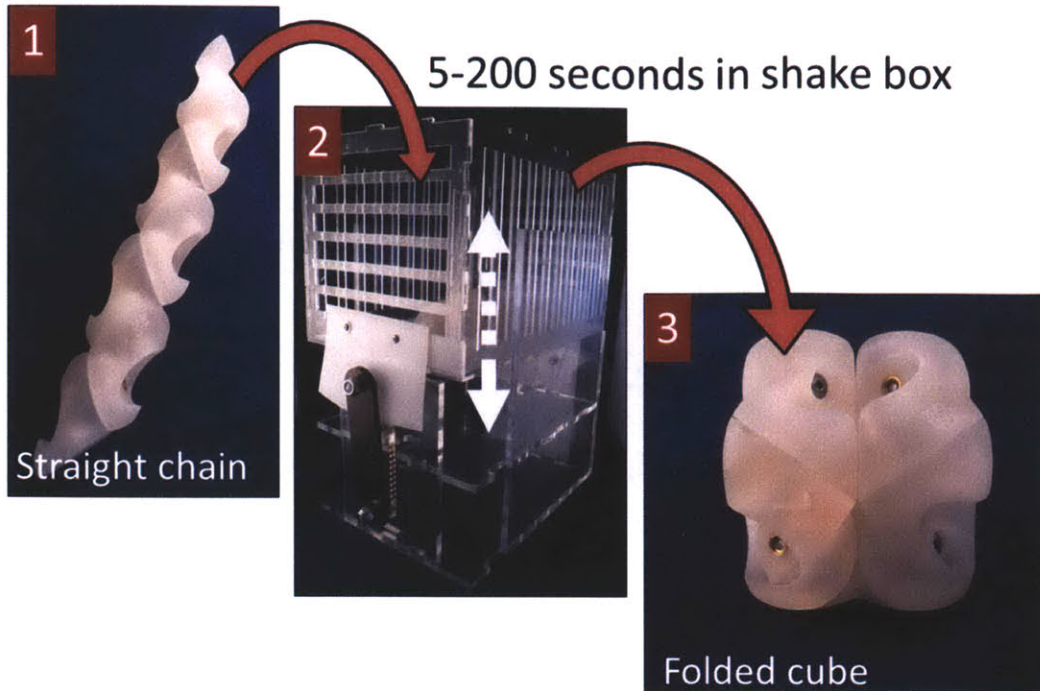


Figure 5.1: Diagram illustrating stochastic folding experiment.

5.1 Description of simulation system

The simulation system uses a framework built by Jonathan Bachrach that uses the Open Dynamics Engine (ODE) for physics simulation and OpenGL for rendering. ODE uses a relaxation type algorithm to simulate rigid body interactions. Prior to settling on this system, we also explored using the Unreal Engine (PhysX physics engine) and Blender Game Engine (Bullet physics engine). Though these systems were quite easy to get started with, we found that because they are both designed for building games, they did not easily provide sufficient low-level access to certain parameters.

Jonathan Bachrach's framework primarily provides a system that quickly allows for instantiating a physics setup with visualization provided by OpenGL. The physics system is done directly through calls to ODE.

The parameters common to all of our simulations are given in Table 5.1. Note that the physics simulation has no inherent units and it is up to the user to use consistent units. It is recommended to use a unit system that keeps masses and lengths in the range of 1-10 [26]. For all of this work, the units correspond to a centimeter, gram and second system (CGS).

Table 5.1: Key parameters of the simulation

Parameter	Value
World update function	dWorldQuickStep, 20 iterations
Mass of node	15
Length of node	2
Gravity	-981
“Bounciness” factor	0.2
Amplitude of shaking	Varies, 1–10
Frequency of shaking	Varies, 1–10

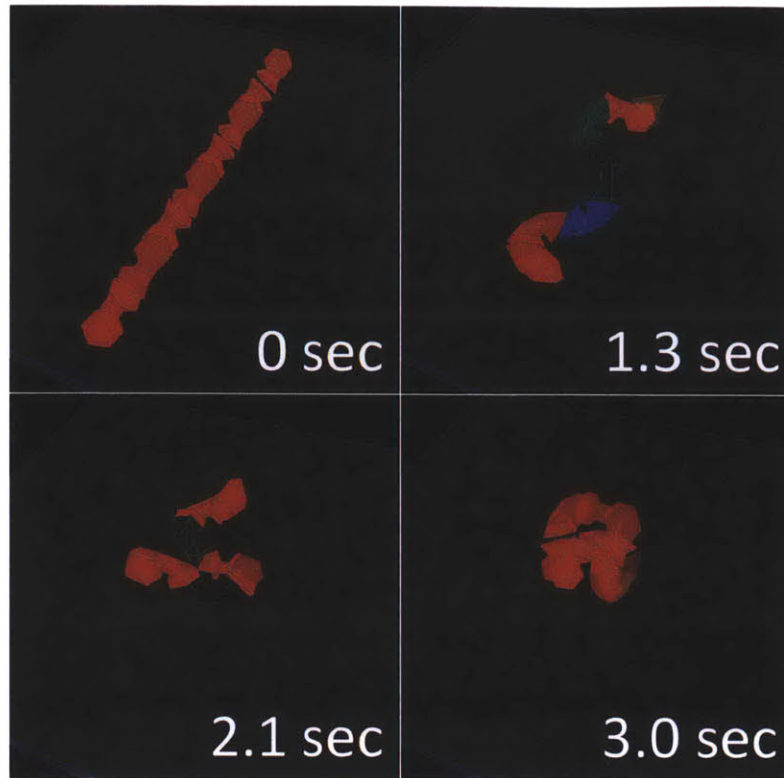


Figure 5.2: Screen captures of a run of the folding simulation. The color indicates how far a node is from its target position.

Additionally, we wrote a short Python script that allows us to queue up many simulations to do parameter sweeps and average data and also issues multiple simultaneous simulations to take advantage of multi core machines. Simulations typically ran at about 6 times faster than simulated time. Screen captures from a run of the simulation are shown in Figure 5.2.

5.2 Description of mechanical system

To conduct the hardware tests, we used the single-position latching chain system described in Section 4.2.3. Though the original goal was to use the one-way bearing system described in Section 4.2.1, this system lacked the robustness and ease of assembly to survive sufficient trials of chains of sufficient length. But, we believe that

it would be possible to construct a similar one-way bearing system that would meet if not exceed the robustness of the latching system used.

Additionally, we constructed a machine to tumble our chains in a repeatable manner. This machine, shown in Figure 5.3, used a crank mechanism to move a box in the vertical direction in an approximately sinusoidal pattern. The amplitude and frequency could be controlled by changing the adjustable pin in the crank and by varying the voltage input to the motor. The frequency was measured by counting the number of cycles over a period of time.

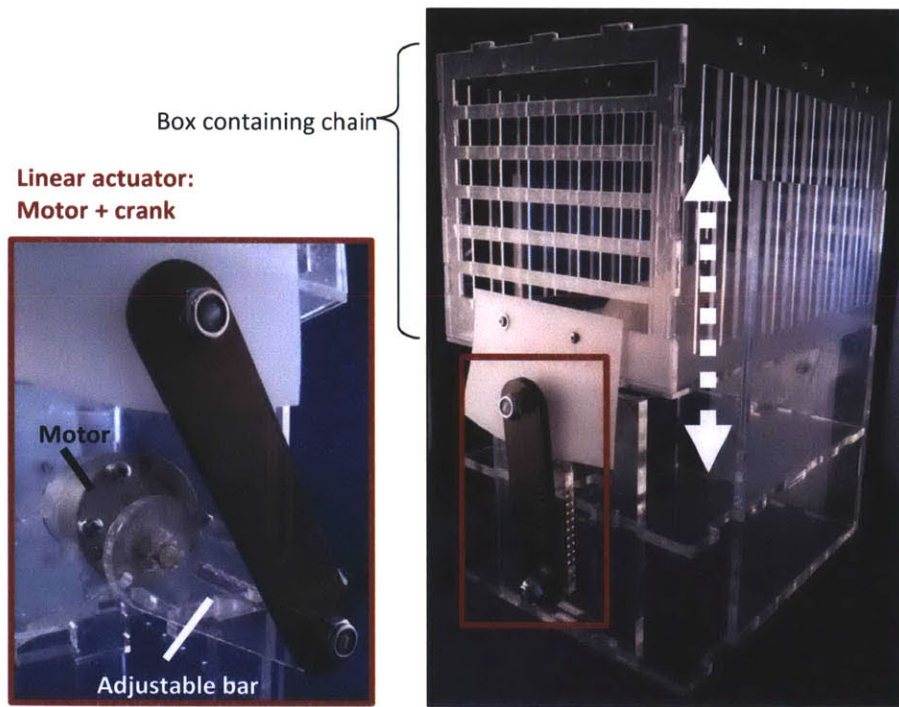


Figure 5.3: Photograph of the shake box set-up, highlighting the motor-driven actuation mechanism.

For all tests, the chain was placed in the box in a straight line configuration prior to starting the shaking. The motor was turned on and a timer started. When the chain appeared to be done folding, the timer was stopped, and the data was used if the chain was confirmed to be folded correctly. All tests were halted at 240 seconds and the chain was assumed to be stuck in a local minima from which it would not escape.

5.3 Configuration

Before we can delve into the other parameters affecting stochastic folding, we must mention that many of the later results may be dependent on the specific configuration of the folds. To examine this, we looked at two basic fold configurations that are as far apart in folded configuration, and also far apart in configuration space of the folds. These are the “cubic” and “spiral” configurations shown in Figure 5.4.



Figure 5.4: CAD models showing “cubic” fold geometry on left and “spiral” geometry on right.

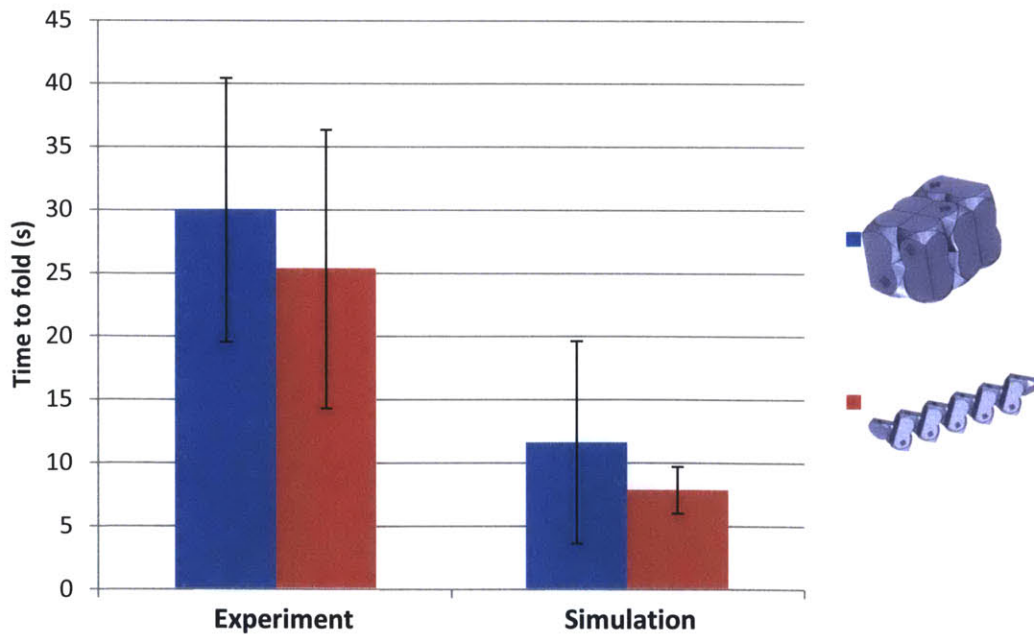


Figure 5.5: Plot showing fold time versus fold geometry in experiment and simulation.

The results of this comparison, shown in Figure 5.5, was that the spiral and cube configuration had comparable fold times. This result was somewhat unexpected as observation of the tumbling motions of these two shapes suggested that the cube would have more difficulty in successfully imparting energy into some nodes when it was partially folded. But, by other analysis, this is the expected result. As both of these shapes have only fully folded joints, they are equally far from the starting position in configuration space. Additionally, at the relatively short lengths examined, shape may not yet have come into play.

5.4 Length

Perhaps the most important parameter to explore is the length of a chain that can be successfully folded and how long it takes to fold such a chain.

First, we tested in simulation and experiment the single-latch system (corresponding to a ratchet increment of 4 radians). Figure 5.6 shows the results of this experiment. The absolute experimental versus simulation time differ significantly. From observing both simulation and experiment, this seems to be caused by an increased stickiness in the physical simulation, not accurately modeled by friction in the simulation. This causes the experimental setup to go through repeated bounces without changing configuration. In both cases, the time sharply rises at approximately four folds. This is the point at which it becomes likely to repeatedly bounce in a configuration without making progress.

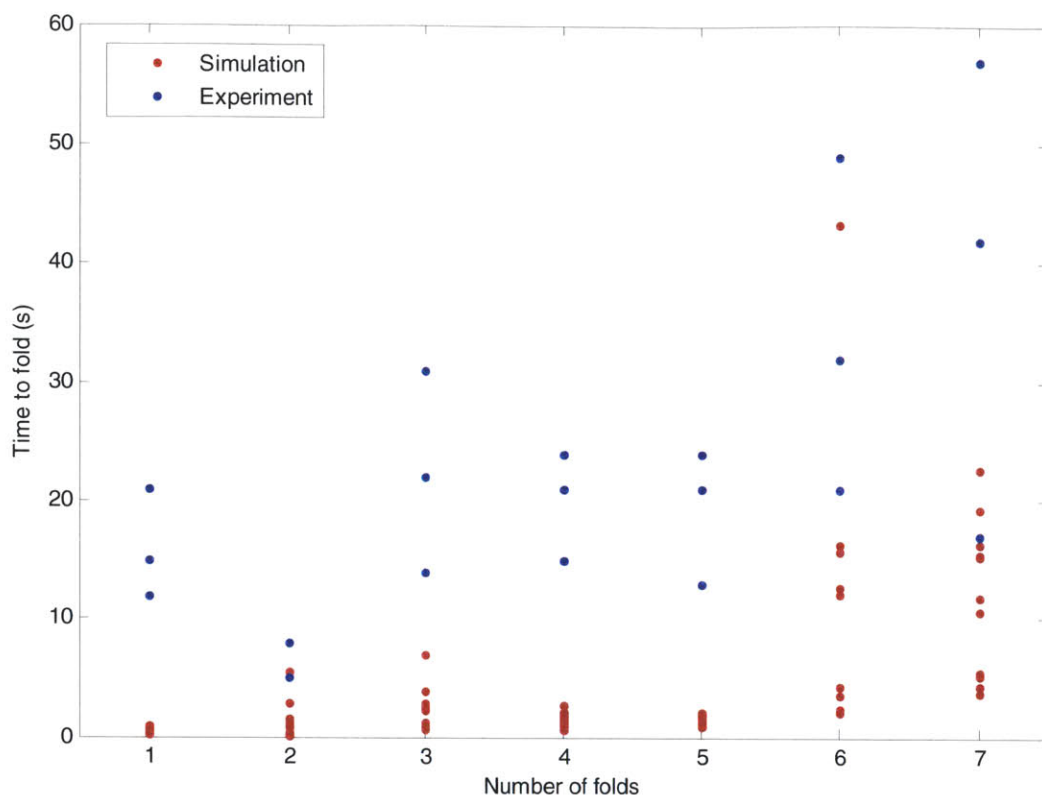


Figure 5.6: Study of fold time versus number of joints folded. Each point represents a single experiment where an unfolded chain is agitated until it is completely folded. Simulated tests are in blue and experimental tests are in red.

Next, we conducted a two parameter study in simulation to see how the ratchet increment size and length affect the maximum length of chain that will successfully fold in simulation. The results are provided in Figure 5.6. One important thing to note from this chart is that decreasing the ratchet increment increases the length of chain that can be folded.

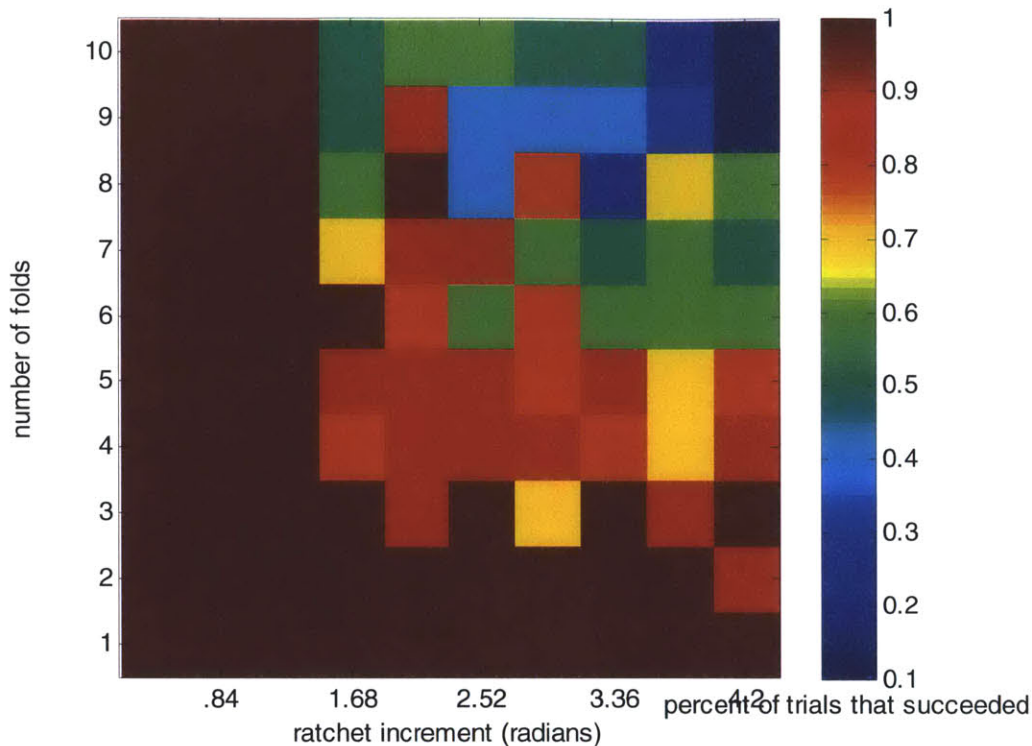


Figure 5.7: Ratchet increment size and chain length versus fraction of trials that succeed in simulation.

In simulation, the absolute longest chain that would fold reliably (at least 9 out of 10 trials succeed) was four folds for the maximum ratchet increment size and was at least 22 for small ratchet sizes (0.42 radians). For the small ratchet increment tests, this was limited by the maximum length we were able to reliably simulate. At longer lengths, the nodes would begin to self-intersect, breaking the accuracy of the simulation.

5.5 Amplitude and frequency

The amplitude and frequency that the system is agitated with obviously have a large effect on performance of the folding process. To begin with, the peak acceleration of the agitation must exceed the acceleration due to gravity to induce any kind of motion in the chain. Beyond that, one might expect there to be an ideal frequency or amplitude to excite motion in the chain. Figure 5.8 shows a two-parameter study looking at the

effect of frequency and amplitude of agitation on fold time. The black lines are contour lines of constant peak acceleration. White areas have no data. The unusual shape of the data region comes from the fact that the two parameters varied in the study were peak acceleration and amplitude, which map onto the plot in this fashion. The area that appears to have the lowest peak acceleration for the fastest times is somewhere around an amplitude of 4-6 and a frequency of 4-6. From observations of the simulation, this makes sense because this amplitude corresponds to motion where the chain is launched in the air just enough to allow free motion of the joints without excessive time in free fall where little movement happens.

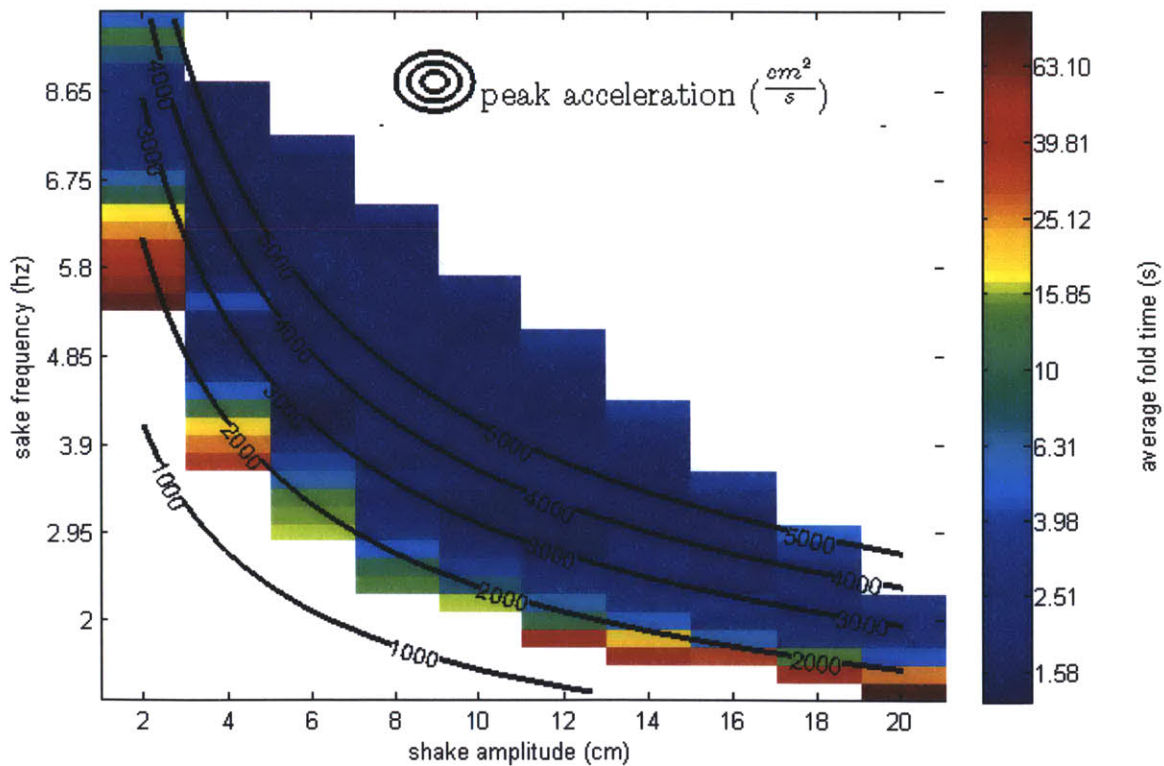


Figure 5.8: Plot showing folding time versus shake frequency and amplitude. Peak acceleration of the shaking motion is shown with contour lines. Note that time is in a logarithmic scale.

6.1 Brownian rectification for programmable matter

We have demonstrated an implementation of Brownian rectification in programmable matter. This allows us to simplify our programmable matter system by removing the major energy input mechanism from the programmable matter system. This comes at a cost in the functionality of the system, but it represents a new region in the complexity-functionality space that may be useful. In particular, this will prove more useful as these systems are scaled down and become increasingly affected by unavoidable noise and thermal energy in their environment.

6.2 Passive ratcheting chains

We primarily explored the simplest possible Brownian rectification mechanism for programmable matter: passive ratchets programmed ahead of time with the desired configuration. This allows making very simple nodes with as few as two or three parts compared to the part counts on the order of 100 for active systems. We were able to fold chains at speeds comparable to the smallest active Moteins built to date, on the order of 60 seconds to a complete system. Additionally, we were able to fold chains as long as the longest active systems folded to date, approximately 10 nodes. However, we showed that there is a limit to the length of the chains of somewhere around 15 nodes, as they begin to get stuck in local minimums caused by self-intersection during the fold. This can be remedied by using smaller ratchet increments.

6.3 Future work

One obvious direction for future work is to push the limits of miniaturization of these ratchet systems. Because they are so simple, it should be possible to fabricate truly small versions (several mm pitch length). These would have the benefits of being able to fold faster and being more robust for a given number of nodes.

Having seen the limitations of passive systems, the next step is to fill in the main remaining space in the continuum of active to passive chain programmable matter: the smart clutch system. Though this now adds the complexity of communication and a simple actuator, it will still be simpler than the actuated system while achieving nearly the same level of control. There are a number of promising materials-based actuators that can lend themselves to this application. In particular, dielectric elastomers and micro-hydraulics are appropriate. We would also expand our simulation system to handle the smart clutch system. The main difficulty here will not be implementing this change, but getting the simulation to run robustly and quickly with the larger number of nodes that we would like to simulate.

Another interesting direction to pursue is to apply this rectification mechanism to a wider range of programmable matter such as sheet and volume geometries that other groups have explored. Though the specific techniques reviewed in this work may not translate directly very well, the basic principle of rectifying random motion has potential.

Finally, a more theoretical direction would be to examine how this system behaves as it is miniaturized and approaches thermal equilibrium. What are the limits in terms of miniaturization or increasing the “temperature” of the vibrations? What is the Feynman-Smulchowski limit where it stops working?

REFERENCES

- [1] K. Cheung, M. Lobovsky and A. Knaian, "Millibiology," MIT Center for Bits and Atoms, 2009. [Online]. Available: <http://milli.cba.mit.edu/>. [Accessed 5 August 2011].
- [2] K. Cheung, E. D. Demaine, J. Bachrach and S. Griffith, "Programmable Assembly with Universally Foldable Strings," *unpublished*, 2010.
- [3] H. P. G. A. C. David W. Oxtoby, Principles of modern chemistry, Cengage Learning, 2007.
- [4] M. Krishnan, M. T. Tolley, H. Lipson and D. Erickson, "Hydrodynamically tunable affinities for fluidic assembly.," *Langmuir : the ACS journal of surfaces and colloids*, vol. 25, no. 6, pp. 3769-74, apr, 2009.
- [5] "File:Maxwell's demon.svg," Wikimedia Foundation, 2 February 2007. [Online]. Available: http://en.wikipedia.org/wiki/File:Maxwell%27s_demon.svg. [Accessed 5 August 2011].
- [6] R. Fox, "Rectified Brownian movement in molecular and cell biology," *Physical Review E*, vol. 57, no. 2, pp. 2177-2203, feb, 1998.
- [7] R. Fox and M. Choi, "Rectified Brownian motion and kinesin motion along microtubules," *Physical Review E*, vol. 63, no. 5, pp. 1-12, apr, 2001.
- [8] R. D. Astumian, "Thermodynamics and Kinetics of a Brownian Motor," *Science*, vol. 276, no. 5314, pp. 917-922, may, 1997.
- [9] R. P. Feynman, The Feynman lectures on physics: Volume 1, Addison-Wesley, 1977.
- [10] P. Eshuis, K. van der Weele, D. Lohse and D. van der Meer, "Experimental Realization of a Rotational Ratchet in a Granular Gas," *Physical Review Letters*, vol. 104, no. 24, pp. 1-4, jun, 2010.
- [11] B. Koivisto, "File:Feynman ratchet.png," 14 July 2007. [Online]. Available: http://en.wikipedia.org/wiki/File:Feynman_ratchet.png. [Accessed 2 August 2011].
- [12] M. Yim, "Modular Self-Reconfigurable Robot Systems," *IEEE Robotics & Automation Magazine*, 2007.

- [13] V. Zykov, A. Chan and H. Lipson, "Molecubes: An Open-Source Modular Robotics Kit," *Proc. IROS*, 2007.
- [14] A. Knaian, "Electropermanent magnetic connectors and actuators: devices and their application in programmable matter," 2010.
- [15] S. T. Griffith, "Growing machines," 2004.
- [16] E. Hawkes, B. An, N. M. Benbernou, H. Tanaka, S. Kim, E. D. Demaine, D. Rus and R. J. Wood, "Programmable matter by folding," *Proceedings of the National Academy of Sciences*, vol. 107, no. 28, pp. 12441-12445, 2010.
- [17] I. Hunter, "Artificial Muscle Technology: Physical Principles and Naval Prospects," *IEEE Journal of Ocean Engineering*, pp. 706-728, 2004.
- [18] R. Pelrine, R. Kornbluh, Q. Pei and J. Joseph, "High-speed electrically actuated elastomers with strain greater than 100%," *Science*, vol. 287, no. 5454, pp. 836-9, 2000.
- [19] F. Carpi, C. Salaris and D. D. Rossi, "Folded dielectric elastomer actuators," *Smart Materials and Structures*, vol. 16, no. 2, pp. S300-S305, 2007.
- [20] C. G. Cameron and M. S. Freund, "Electrolytic actuators: alternative, high-performance, material-based devices," *Proceedings of the National Academy of Sciences of the United States of America*, vol. 99, no. 12, pp. 7827-31, 2002.
- [21] N. Cheng, G. Ishigami, S. Hawthorne, H. Chen, M. Hansen, M. Telleria, R. Playter and K. Iagnemma, "Design and analysis of a soft mobile robot composed of multiple thermally activated joints driven by a single actuator," (*ICRA*), *2010 IEEE*, pp. 5207-5212, 2010.
- [22] M. Telleria, M. Hansen, D. Campbell, A. Servi and M. L. Culpepper, "Modeling and implementation of solder-activated joints for single-actuator, centimeter-scale robotic mechanisms," in *IEEE International Conference on Robotics and Automation*, 2010.
- [23] J. Yang, Y. Huang, J. Ho, W. Sun, H. Huang, Y. Lin, S. Huang, S. Huang, H. Lu and I. Chao, "A pentaptycene-derived light-driven molecular brake," *Organic Letters*, vol. 10, no. 11, pp. 2279-2282, 2008.
- [24] J. Nottelmann, "Sensor-less Rotation Counting in Brush Commutated DC motors," 2010.
- [25] J. Bachrach, V. Zykov and S. Griffith, "Folding Arbitrary 3D Shapes with Space Filling Chain Robots : Reverse Explosion Approach to Folding Sequence Design," *unpublished*.

- [26] "HOWTO make the simulation better," 23 March 2011. [Online]. Available: http://opende.sourceforge.net/wiki/index.php/HOWTO_make_the_simulation_better. [Accessed 4 August 2011].
- [27] S. Klein, "Orange Fly," 18 September 2010. [Online]. Available: <http://www.flickr.com/photos/adamentmeat/5002565607/>. [Accessed 4 August 2011].
- [28] R. Gross and M. Dorigo, "Self-Assembly at the Macroscopic Scale," *Proceedings of the IEEE*, vol. 96, no. 9, pp. 1490-1508, 2008.
- [29] Y. Chen, J. Chang, A. Greenlee, K. Cheung, A. Slocum and R. Gupta, "Multi-turn, tension-stiffening catheter navigation system," in *Robotics and Automation (ICRA), 2010 IEEE International Conference on*, 2010.